Inorganic Chemistry
Article

Inorg. Chem. **2010**, *49*, 7289–7297 **7289**
DOI: 10.1021/ic902346u

Trimethylsilylchalcogenolates of Co(II) and Mn(II): From Mononuclear Coordination Complexes to Clusters Containing $-ESiMe_3$ Moieties (E = S, Se)

Chhatra B. Khadka,[†] Daniel G. Macdonald,[†] Yanhua Lan,[‡] Annie K. Powell,[‡] Dieter Fenske,[‡] and John F. Corrigan*,[†]

[†]*Department of Chemistry, The University of Western Ontario, London, Ontario, N6A 5B7 Canada, and* [‡]*Institut für Anorganische Chemie, Unversität Karlsruhe, D 76128 Karlsruhe, Germany*

Received November 26, 2009

The Co(II) and Mn(II) complexes (tmeda)$Co(ESiMe_3)_2$ (E = S, **1a**; E = Se, **1b**), $(3,5\text{-}Me_2C_5H_3N)_2Co(ESiMe_3)_2$ (E = S, **2a**; E = Se, **2b**), $[Li(tmeda)]_2[(tmeda)Mn_5(\mu\text{-}ESiMe_3)_2(ESiMe_3)_4(\mu_4\text{-}E)(\mu_3\text{-}E)_2]$ (E = S, **3a**; E = Se, **3b**), $[Li(tmeda)]_2[Mn(SSiMe_3)_4]$ (**4**), $[Li(tmeda)]4[Mn_4(SeSiMe_3)_4(\mu_3\text{-}Se)_4]$ (**5**), and $[Li(tmeda)]_4[Mn(Se_4)_3]$ (**6**) (tmeda = *N*,*N*,*N*′,*N*′-tetramethylethylenediamine) have been isolated from reactions of $Li[ESiMe_3]$ and the chloride salts of these metals. The treatment of $(tmeda)CoCl_2$ with two equivalents of $Li[ESiMe_3]$ (E = S, Se) yields **1a** and **1b**, respectively, whereas similar reactions with $MnCl_2$ yield the polynuclear complexes **3a** (E = S) and **3b** (E = Se). The selective preparation of the mononuclear complex **4** is achieved by increasing the reaction ratios of $Li[SSiMe_3]$ to $MnCl_2$ to 4:1. Single crystal X-ray analysis of complexes **1**−**5**, confirms the presence of the trimethylsilylchalcogenolate moieties and distorted tetrahedral geometry around the metal centers in each of these complexes. The structure of the tris(tetraselenide) complex $[Li(tmeda)]_4[Mn(Se_4)_3]$ (**6**), isolated in small quantities from the preparation of **5**, is also described.

Introduction

Despite the continued interest in the fundamental chemistry of polynuclear heterometallic chalcogen nanometer-sized clusters, the chemistry of ternary MM′E systems remains underdeveloped relative to binary systems. This is due in part to a lack of general synthetic routes and suitable, stable precursors, although this area of research is burgeoning rapidly.[1] Metal chalcogenolate complexes of the d-block metals with trimethylsilyl functionalities on the chalcogen centers have recently successfully been utilized as precursors for the synthesis of ternary MM′E clusters. The preformed metal−chalcogen bond and high solubility of these complexes in common organic solvents, coupled with the reactivity of the $-ESiMe_3$ (E = S, Se, Te) ligands toward (ligand stabilized) metal salts, makes these complexes powerful precursors for the formation of M−E−M′ bonding interactions and entry into ternary d-block metal MM′E clusters.[2−9] Using these reagents as sources of soluble, protected "metallachalcogenolates" (metal-chalcogenides), the ternary nanoclusters $[Cu_{20}Hg_{15}E_{25}(P^nPr_3)_{18}]$ (E = S, Se),[2a] $[Zn_xCd_{10-x}E_4(EPh)_{12}(P^nPr_3)_4]$ (E = Se, Te),[4] and $[Cu_9Ag_3S_6(PEtPh_2)_8]$[9] have been successfully synthesized using $(P^nPr_3)_3Cu(ESiMe_3)$, $(3,5\text{-}Me_2C_5H_3N)_2Zn(ESiMe_3)_2$, and $(PEtPh_2)_3Cu(SSiMe_3)$, respectively. The successful synthesis of heterometallic ternary complexes can be achieved using complexes with less steric

*Corresponding author. To whom correspondence should be addressed. E-mail: corrigan@uwo.ca.

(1) (a) Zhang, Q. F.; Leung, W. H.; Xin, X. *Coord. Chem. Rev.* **2002**, *224*, 35–49. (b) DeGroot, M. W.; Corrigan, J. F. *Comprehensive Coordination Chemistry II*; Fujita, M., Powell, A., Creutz, C., Eds.; Elsevier: Oxford, U. K., 2004; Vol. *7*, pp 57−113. (c) DeGroot, M. W.; Corrigan, J. F. *The Chemistry of Nanomaterials: Synthesis, Properties and Applications*; Rao, C. N. R., Muller, A., Cheetham, A. K., Eds; Wiley-VCH: Weinheim, Germany, 2004; Vol. *2*, pp 418−451. (d) Dehnen, S.; Eichhöfer, A.; Fenske, D. *Eur. J. Inorg. Chem.* **2002**, *2*, 279–317. (e) Efros, A. I.; Rosen, M. *Annu. Rev. Mater. Sci.* **2000**, *30*, 475–521. (f) Hou, H.-W.; Xin, X.-Q.; Shi, S. *Coord. Chem. Rev.* **1996**, *153*, 25–56. (g) Dehnen, S.; Melullis, M. *Coord. Chem. Rev.* **2006**, *251*, 1259–1280.

(2) (a) Tran, D. T. T.; Taylor, N. J.; Corrigan, J. F. *Angew. Chem., Int. Ed. Engl.* **2000**, *39*, 935–937. (b) Tran, D. T. T.; Beltran, L. M.; Kowalchuk, C. M.; Trefiak, N. R; Taylor, N. J.; Corrigan, J. F. *Inorg. Chem.* **2002**, *41*, 5693–5698.

(3) DeGroot, M. W.; Taylor, N. J.; Corrigan, J. F. *J. Mater. Chem.* **2004**, *14*, 654–660.

(4) DeGroot, M. W.; Taylor, N. J.; Corrigan, J. F. *Inorg. Chem.* **2005**, *44*, 5447–5458.

(5) (a) DeGroot, M. W.; Corrigan, J. F. *Angew. Chem., Int. Ed.* **2004**, *43*, 5355–5357. (b) DeGroot, M. W.; Taylor, N. J; Corrigan, J. F. *J. Am. Chem. Soc.* **2003**, *125*, 864–865.

(6) (a) Komuro, T.; Matsuo, T.; Kawaguchi, H.; Tatsumi, K. *J. Chem. Soc., Dalton Trans.* **2004**, *10*, 1618–1625. (b) Komuro, T.; Matsuo, T.; Kawaguchi, H.; Tatsumi, K. *J. Chem. Commun.* **2002**, *9*, 988–989. (c) Komuro, T.; Matsuo, T.; Kawaguchi, H.; Tatsumi, K. *Angew. Chem., Int. Ed.* **2003**, *42*, 465–468.

(7) (a) Sommer, H.; Eichhöfer, A.; Drebov, N.; Ahlrichs, R.; Fenske, D. *Eur. J. Inorg. Chem.* **2008**, *32*, 5138–5145. (b) Bechlars, B.; Issac, I.; Feuerhake, R.; Clerac, R.; Fuhr, O.; Fenske, D. *Eur. J. Inorg. Chem.* **2008**, *10*, 1632–1644. (c) Feuerhake, R.; Fenske, D. *Z. Anorg. Allg. Chem.* **2003**, *629*, 2317–2324.

(8) DeGroot, M. W.; Corrigan, J. F. *Z. Anorg. Allg. Chem.* **2006**, *632*, 19–29.

(9) Borecki, A.; Corrigan, J. F. *Inorg. Chem.* **2007**, *46*, 2478–2484.

Published on Web 07/21/2010

demands about the chalcogen centers (e.g., $[SSiMe_2S^{2-}]$[6b,c] or $-SiMe_3{}^{2-5}$), as larger substituents about the silicon centers can result in nonselective M−E/E−Si bond cleavage reactions.[6a] The demonstrated ability of these trimethylsilylchalcogenolates as molecular precursors to ternary MM′E nanoclusters and nanoparticles has prompted us to expand this class of complexes to include the paramagnetic metal ions Mn(II) and Co(II). Herein, we report the synthesis and structural characterization of a set of manganese and cobalt trimethylsilylchalcogenolates stabilized with 3,5-lutidine and *N*,*N*,*N*′,*N*′-tetramethylethylenediamine ligands: $(tmeda)Co(ESiMe_3)_2$ (E = S, **1a**; E = Se, **1b**), $(3,5\text{-}Me_2C_5H_3N)_2Co(ESiMe_3)_2$ (E = S, **2a**; E = Se, **2b**), $[Li(tmeda)]_2[(tmeda)Mn_5(\mu\text{-}ESiMe_3)_2(ESiMe_3)_4(\mu_4\text{-}E)(\mu_3\text{-}E)_2]$ (E = S, **3a**; E = Se, **3b**), $[Li(tmeda)]_2[Mn(SSiMe_3)_4]$ (**4**), $[Li(tmeda)]_4[Mn_4(SeSiMe_3)_4(\mu_3\text{-}Se)_4]$ (**5**).

Experimental Section

All experimental procedures were performed using standard double manifold Schlenk line techniques under an atmosphere of dried nitrogen gas or in nitrogen filled glove boxes. The nonchlorinated solvents (THF, hexanes) were dried and collected using an MBraun MB-SP Series solvent purification system with tandem activated alumina (THF) and activated alumina or an activated copper redox catalyst (hydrocarbons).[10] CH_2Cl_2 was dried and distilled over P_2O_5. tmeda and 3,5-lutidine were dried and distilled over CaH_2 and Na, respectively. $MnCl_2$ and $CoCl_2$ were purchased from Aldrich in 98% purity and used as supplied. The 1.6 M ^nBuLi in hexanes was purchased from Aldrich. The silylated reagents $E(SiMe_3)_2$ (E = S, Se) were synthesized using literature procedures.[3,11] $Li[ESiMe_3]$ (E = S, Se) was prepared following a previously published literature procedure.[12]

X-ray data were collected on Enraf-Nonius Kappa-CCD and Bruker-APEX-II (**3a** and **3b**) diffractometers equipped with graphite-monochromated Mo Kα (λ = 0.71073 Å) radiation. Single crystals of the complexes were carefully selected, immersed in paraffin oil, and mounted on a nylon loop. Crystals were placed in a cold stream of N_2 to prevent decomposition. The structures were solved using direct methods and refined by the full-matrix least-squares procedure of SHELXTL (G. M. Sheldrick, Madison,WI, 1996). With the exception of disordered carbon atoms of the tmeda ligands and $-SiMe_3$ substitutents, all non-hydrogen atoms were refined anisotropically, while hydrogen atoms were kept at their calculated distances and refined using a riding model. For **4**, satisfactory refinement of the data was completed with the resolution of a TWIN component (*k*, *h*, −*l*) and resultant BASF values 0.16690 and 0.12390.

The magnetic susceptibility measurements of solid samples **3a**, **3b**, and **5** were carried out with the use of a Quantum Design SQUID MPMS-XL magnetometer. This magnetometer works between 1.8 and 400 K for DC applied fields ranging from −7 to +7 T. AC susceptibility measurements can be measured with an oscillating AC field of 3 Oe and AC frequencies ranging from 1 to 1500 Hz. *M* vs *H* measurements were performed at 100 K to check for the presence of ferromagnetic impurities in all cases. The magnetic data were corrected for the sample holder and the diamagnetic contribution. AC susceptibility measurements have been checked with an oscillating AC field of 3 Oe and AC frequencies at 1000 Hz. Measurements were performed on a polycrystalline sample of 12.5 mg (**3a**), 5.6 mg (**3b**), and 31.4 mg (**5**), respectively. The sample bags were prepared in a glovebox and measured immediately. It is worth pointing out that the complexes are very air sensitive. Sample bags for SQUID measurements were prepared in a glovebox; however noticeable color changes of the samples on transferring the bags into SQUID suggest there may be some partial oxidation.

Elemental analysis of **2a**, **3a**, **3b**, and **4** was performed by Guelph Chemical Laboratories, Ltd. (Ontario, Canada) and by Columbia Analytical Services (Tucson, Arizona) for **5** and **6**. Due to the highly air sensitive nature of **1a**, **1b**, and **2b**, elemenal analyses were not possible. Sample homogeneity was determined via unit cell measurements on random samplings of the single crystals obtained.

Synthesis of $(tmeda)Co(SSiMe_3)_2$ (1a). $CoCl_2$ (0.173 g, 1.33 mmol) was dissolved in 20 mL of CH_2Cl_2 by adding tmeda (0.30 mL, 2.00 mmol) to yield a blue solution. This solution was then added to freshly prepared $Li[SSiMe_3]$ (2.84 mmol) at 0 °C. A suspension was obtained after stirring for 1 h and raising the temperature to room temperature. Compound **1a** was purified by the removal of solvent in a vacuum, followed by extraction with hexanes and filtration. Blue needle-like crystals were obtained by reducing the solvent volume by half and storage at −25 °C for a few days. Yield: 0.128 g (25% based on $CoCl_2$). mp 117−120 °C (dec).

Synthesis of $(tmeda)Co(SeSiMe_3)_2$ (1b). $CoCl_2$ (0.139 g, 1.07 mmol) was dissolved in 20 mL of CH_2Cl_2 by adding tmeda (0.25 mL, 1.67 mmol). This solution was then added to freshly prepared $Li[SeSiMe_3]$ (2.30 mmol) at 0 °C. A green suspension was obtained after stirring for 20 min at 0 °C. Compound **1b** was purified in an analogous manner to **1a** and isolated as green crystals. Yield: 0.102 g (20% based on $CoCl_2$). mp 97−98 °C (dec).

Synthesis of $(3,5\text{-}Me_2C_5H_3N)_2Co(SSiMe_3)_2$ (2a). $CoCl_2$ (0.145 g, 1.12 mmol) was dissolved in 30 mL of CH_2Cl_2 by adding 3,5-lutidine (0.40 mL, 3.50 mmol) to yield a blue solution after stirring overnight. This solution was then added to freshly prepared $Li[SSiMe_3]$ (2.37 mmol) at 0 °C. A blue suspension was obtained after stirring for 15 min at 0 °C. Compound **2a** was purified by the removal of solvent in a vacuum, followed by extraction with hexanes and filtration. Blue crystals were obtained by the reduction of solvent and storage at −80 °C in a freezer for a few weeks. Yield: 0.108 g (20% based on $CoCl_2$). Anal. Calcd for $C_{20}H_{36}CoN_2S_2Si_2$: C, 49.66%; H, 7.50%. Found: C, 49.33%; H, 7.24%.

Synthesis of $(3,5\text{-}Me_2C_5H_3N)_2Co(SeSiMe_3)_2$ (2b). $CoCl_2$ (0.147 g, 1.13 mmol) was dissolved in 30 mL of CH_2Cl_2 by adding 3,5-lutidine (0.40 mL, 3.50 mmol), which was then added to freshly prepared $Li[SeSiMe_3]$ (2.30 mmol) at −60 °C. A green suspension was obtained after stirring for 15 min, not allowing the temperature to go above −50 °C. The solution was filtered cold. Green crystals were obtained by the reduction of the solvent volume and storage at −45 °C. Yield: 0.098 g (15% based on $CoCl_2$); mp 106−107 °C (dec).

Synthesis of $[Li(tmeda)]_2[(tmeda)Mn_5(SSiMe_3)_6(S)_3]$ (3a). tmeda (0.24 mL, 1.56 mmol) was added to a suspension of $MnCl_2$ (0.131 g, 1.04 mmol) in 10 mL of CH_2Cl_2 and stirred at room temperature. After stirring for 1 h, a pink suspension was obtained. This suspension was then added to freshly prepared $Li[SSiMe_3]$ (2.08 mmol) at 0 °C and stirred for 2 h while slowly warming to room temperature, to produce an orange-red suspension. The solvent was removed under a vacuum, and the product was extracted with 20 mL of hexanes. Compound **3a** was obtained after filtering the extracted orange-red solution through dried Celite. The volume of the solution was reduced by half and stored at −25 °C for a few days to afford orange-red X-ray quality crystals of **3a**. Yield: 0.152 g (53.5% based on $MnCl_2$). Anal. Calcd for $C_{36}H_{102}Li_2Mn_5N_6S_9Si_6$: C, 31.68%; H, 7.53%. Found: C, 31.98%; H, 7.75%.

Synthesis of $[Li(tmeda)]_2[(tmeda)Mn_5(SeSiMe_3)_6(Se)_3]$ (3b). The synthesis of **3b** was carried out in a similar way as for **3a** by the addition of $MnCl_2$ (0.155 g, 1.23 mmol) and tmeda (0.28 mL, 1.85 mmol) suspended in 10 mL of CH_2Cl_2 to freshly prepared

(10) Pangborn, A. B.; Giardello, M. A; Grubbs, R. H.; Rosen, R. K.; Timmers, F. *J. Organometallics* **1996**, *15*, 1518–1520.
(11) So, J; Boudjouk, P *Synthesis* **1989**, 306–307.
(12) Taher, D; Wallbank, A. I.; Turner, E. A.; Cuthbert, H. L; Corrigan, J. F. *Eur. J. Inorg. Chem.* **2006**, *22*, 4616–4620.

Scheme 1. Synthesis of (tmeda)$Co(ESiMe_3)_2$ (**1**) and $(3,5\text{-}Me_2C_5H_3N)_2$-$Co(ESiMe_3)_2$ (**2**)

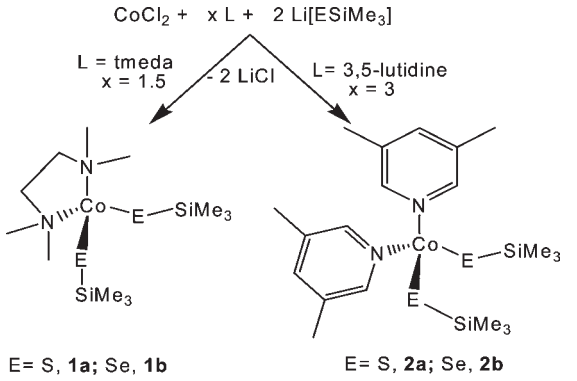

$Li[SeSiMe_3]$ (2.46 mmol). The product **3b** was obtained in the form of orange-red crystals by reducing the volume by half and storing it at −25 °C for a few days. Yield: 0.090 g (20.5% based on $MnCl_2$). Anal. Calcd for $C_{36}H_{102}Li_2Mn_5N_6Se_9Si_6$: C, 24.20%; H, 5.75%. Found: C, 23.67%; H, 5.72%.

Synthesis of $[Li(tmeda)]_2[Mn(SSiMe_3)_4]$ (4). tmeda (0.45 mL, 3.00 mmol) was added to a suspension of $MnCl_2$ (0.151 g, 1.20 mmol) in 20 mL of CH_2Cl_2 and stirred at room temperature. After 1 h of stirring, a pink suspension was obtained. This suspension was then added to freshly prepared $Li[SSiMe_3]$ (4.82 mmol) at 0 °C to form a pale pink colored solution. After removal of the solvent in vacuum, extraction of the residue with hexanes and subsequent filtration over Celite, pale pink crystals were obtained by storing concentrated solutions of **4** at −25 °C for a few days. Yield: 0.347 g (40.0% based on $MnCl_2$). Anal. Calcd for $C_{24}H_{68}Li_2MnN_4S_4Si_4$: C, 39.91%; H, 9.49%. Found: C, 39.79%; H, 9.75%.

Synthesis of $[Li(tmeda)]_4[Mn_4(SeSiMe_3)_4(Se)_4]$ (5) and $[Li(tmeda)]_4[Mn(Se_4)_3]$ (6). tmeda (0.35 mL, 2.33 mmol) was added to a suspension of $MnCl_2$ (0.119 g, 0.946 mmol) in 20 mL of CH_2Cl_2 and stirred at room temperature. After 1 h of stirring, a pink suspension was obtained. This suspension was then added to freshly prepared $Li[SeSiMe_3]$ (3.79 mmol) at 0 °C to form a deep red solution. The solvent was removed in a vacuum, and the residue was extracted with hexanes and filtered over Celite. Two different colored crystals were obtained by reducing the solvent volume and storing the solution at −5 °C for a few days. Orange red crystals were characterized as $[Li(tmeda)]_4$-$[Mn_4(SeSiMe_3)_4(Se)_4]$ (**5**), and dark red/brown crystals were characterized as $[Li(tmeda)]_4[Mn(Se_4)_3]$ (**6**). These could be partially separated by hand. Yield: **5**, 0.153 g (40% based on $MnCl_2$). Yield: **6**, 0.071 g (5% based on $MnCl_2$). Anal. Calcd for $C_{36}H_{100}Li_4Mn_4N_8Se_8Si_4$, **5**: C, 26.40%; H, 6.16%. Found: C, 25.73%; H, 6.16%. Anal. Calcd for $C_{24}H_{64}Li_4MnN_8Se_{12}$, **6**: C, 19.28%; H, 4.31%. Found: C, 20.01%; H, 4.00%

Results and Discussion

Synthesis and Characterization of Cobalt(II) Chalcogenolate Complexes. The cobalt trimethylsilylchalcogenolates **1** and **2** have been prepared by the reaction of $CoCl_2$ with an appropriate nitrogen donor ligand followed by the addition of freshly prepared lithium salts of the trimethylsilylchalcogenolate anion, $Li[ESiMe_3]$, at low temperatures, as illustrated in Scheme 1.

The generation and precipitation of LiCl is the driving force for these reactions, with the resultant formation of metal-chalcogen bonding interactions. Both chalcogenide (E^{2-}) and chalcogenolate (RE^-) ligands tend to adopt bridging coordination modes due to the high polarizability of the chalcogens, which often results in the formation of polynuclear species.[8] To avoid the formation of cluster complexes, the addition of at least 2 equiv of $Li[ESiMe_3]$ to $CoCl_2$ to promote the terminal coordination of the trimethylsilylchalcogenolate ligand and the use of an excess amount of the ligand to favor the formation of monomeric complexes is vital.[13] Complexes **1** and **2** are highly air sensitive; however they can be stored for extended periods as solids at −25 °C under an inert atmosphere. The cobalt trimethylsilylselenolates are thermally less stable than their thiolate analogues, with crystalline tmeda complexes generally being less stable than the related 3,5-lutidine complexes. The differences in the thermal stability of these complexes sulfur vs selenium is consistent with those previously reported for zinc and copper chalcogenolates.[2a,13]

Single-crystal X-ray diffraction data were collected for all complexes, and the analyses confirmed the monomeric nature of the structures. A summary of the crystal data and structural parameters for **1a**, **1b**, **2a**, and **2b** is listed in Table 1. The isomorphous tmeda ligated complexes **1a** and **1b** crystallized in the monoclinic space group $C2/c$ with $Z = 12$. There are two independent molecules in the asymmetric unit, one of which resides around a crystallographic 2-fold rotation axis, whereas the second sits in a general position. Bond lengths and angles refer to the latter. The lutidine complex **2a** crystallizes in orthorhombic space group $Pca2(1)$, while **2b** crystallizes in the triclinic space group $P\bar{1}$. The molecular structures of **1a** and **2b** are shown in Figures 1 and 2, respectively.

It has been demonstrated that the controlled formation of M−E−M′ interactions by the reaction of metal−chalcogenolate complexes $M-ESiR_3$ with other metals salts (M′−X) via the elimination of a soluble silane R_3Si-X is adversely affected with the introduction of more sterically demanding substitutents on Si and optimized with three methyl groups about silicon ($M-ESiMe_3$), balanced by the requirements of a suitably stable precursor that is amenable to further reaction chemistry.[6a] The isolation of the monomeric cobalt chalcogenolate complexes **1** and **2** containing terminal $-ESiMe_3$ substitutents makes them ideal candidates for use as molecular precursors for the controlled synthesis of ternary nanometer sized clusters and particles.[2,4,9] The common structural features prevalent in all four complexes are the distorted tetrahedral geometry at the Co(II) center and the presence of a terminally bonded trimethylsilylchalcogenolate ligand, as depicted in Figures 1 and 2. The tmeda ligands are coordinated in a bidentate manner in complexes **1a** and **1b**, while two 3,5-lutidine ligands complete the tetrahedral coordination geometry about the cobalt center in **2a** and **2b**.

Selected bond distances and angles for complexes **1** and **2** are summarized in Table 2. The "CoE_2N_2" (E = S, Se) core in complexes **1** and **2** is significantly distorted from an ideal tetrahedral geometry with the E1−Co−E2 angle ranging from 123.69(4) to 129.48(7)° and N1−Co−N2 ranging from 86.6(2) to 103.7(2). The N1−Co−N2 angle is significantly smaller for the tmeda ligated complexes than the 3,5-lutidine counterpart. The average Co−S bond distance (2.268(1) Å) is slightly shorter compared to the Co−Se average bond distance of 2.384(1) Å, as

(13) DeGroot, M. W.; Corrigan, J. F. *Organometallics* **2005**, *24*, 3378–3385.

Table 1. Crystallographic Data

	1a	1b	2a	2b	3a	3b	4	5	6
chemical formula	$C_{12}H_{34}CoN_2S_2Si_2$	$C_{12}H_{34}CoN_2Se_2Si_2$	$C_{20}H_{36}CoN_2S_2Si_2$	$C_{20}H_{36}CoN_2Se_2Si_2$	$C_{36}H_{102}Li_2Mn_5N_6S_9Si_6\cdot(C_6H_{14})_{1.15}$	$C_{36}H_{102}Li_2Mn_5N_6Se_9Si_6\cdot C_6H_{14}$	$C_{24}H_{68}Li_2MnN_4S_4Si_4$	$C_{36}H_{100}Li_4Mn_4N_8Se_8Si_4$	$C_{24}H_{64}Li_4MnN_8Se_{12}$
fw	385.64	479.44	483.74	577.54	1463.99	1873.17	722.24	1636.80	1495.05
space group	*C*2/*c*	*C*2/*c*	*Pca*2(1)	$P\bar{1}$	*P*2(1)/*c*	*C*2/*c*	*P*4(1)	$P\bar{1}$	*P*2(1)/*n*
temp (K)	150(2)	150(2)	150(2)	150(2)	150(2)	150(2)	150(2)	150(2)	150(2)
a (Å)	25.068(1)	25.487(2)	16.961(4)	9.0799(4)	16.7280(8)	16.6855(9)	11.1899(3)	12.1008(3)	18.8776(8)
b (Å)	14.3286(7)	14.465(1)	8.704(2)	9.9145(5)	17.8065(8)	18.3900(9)		14.1392(4)	14.5127(4)
c (Å)	18.7037(9)	18.835(1)	17.945(5)	16.6353(6)	29.6483(15)	26.4291(15)	35.457(1)	22.2136(6)	19.4562(8)
α (deg)				95.734(2)				99.701(1)	
β (deg)	105.225(2)	104.930(3)		91.369(2)	93.000(1)	91.341(1)		90.315(2)	108.08(2)
γ (deg)				115.881(2)				104.171(1)	
V (Å ^{3})	6482.4(5)	6709.5(8)	2649.2(11)	1336.8(1)	8819.2(7)	8107.5(7)	4439.7(2)	3628.0(2)	5067.1(3)
μ (mm^{-1})	1.091	4.122	0.904	3.462	1.020	4.915	0.621	4.787	8.906
Z	12	12	4	2	4	4	4	2	4
ρ (g cm^{-3})	1.185	1.424	1.213	1.435	1.145	1.535	1.081	1.498	1.960
data/params	5732/273	5922/273	3851/254	6176/253	15509/627	8592/318	6117/362	16647/604	11633/442
R_1 [$I > 2\sigma(I)$]	0.0584	0.0537	0.0575	0.0461	0.0480	0.0505	0.0398	0.0534	0.0695
wR_2[$I > 2\sigma(I)$]	0.1431	0.1127	0.1079	0.1194	0.1452	0.1003	0.0904	0.1208	0.1669

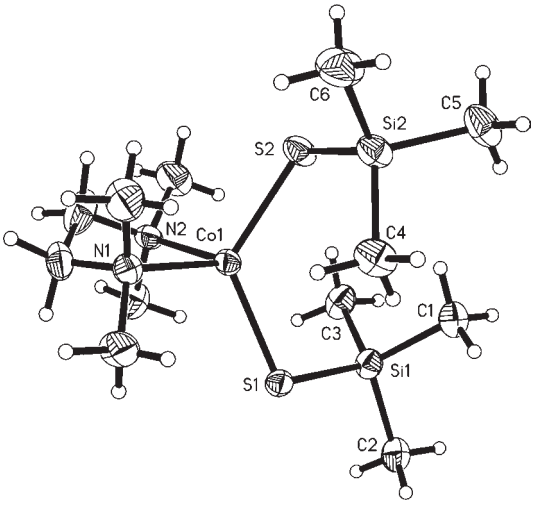

Figure 1. Molecular structure of (tmeda)Co($SSiMe_3$)$_2$ (**1a**) in the crystal (molecule 1). Thermal ellipsoids are drawn at 35% probability. The numbering used for **1b** is similar.

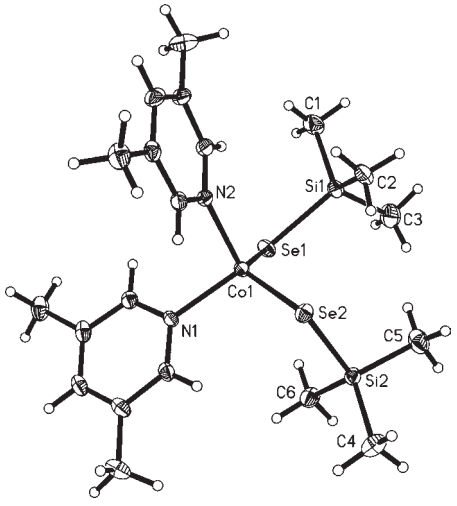

Figure 2. Molecular structure of (3,5-$Me_2C_5H_3N$)$_2$Co($SeSiMe_3$)$_2$ (**2b**) in the crystal. Thermal ellipsoids are drawn at 35% probability. The numbering for **2a** is similar.

expected. The same trend is observed for the E−Si bond distances (Table 2). The bond angles and distances observed for **1a** are comparable to those previously reported for the four coordinate cobalt thiolato complexes (tmeda)Co($SSiPh_3$)$_2$[14] and (tmeda)Co($SSiMe_2Bu^t$)$_2$[6a], and those observed for **2a** are comparable to the previously reported pyridine (py) stabilized cobalt thiolate complex (py)$_2$Co(S-2,4,6-Pr$i_3C_6H_2$)$_2$.[15]

Similar reaction strategies as used for the preparation of mononuclear complexes **1** and **2** with the manganese salt $MnCl_2$ do not result in the isolation of structurally related complexes. The reaction of $MnCl_2$(tmeda)[16] with two equivalents of Li[$ESiMe_3$] led to a dark orange colored solution almost immediately upon mixing, and the isolation of the pentanuclear manganese chalcogenolate complexes [Li(tmeda)]$_2$[(tmeda)Mn_5($ESiMe_3$)$_6$(E)$_3$], **3a** (E = S) and **3b** (E = Se). The yields for **3a** and **3b** were ultimately optimized by varying the ratios of reagents according to eq 1. The tetrameric nature of $MnCl_2$(tmeda) and the relative lability of the N-donor ligands for the d^5 metal ion together with the preferred bridging coordination modes of the chalcogen presumably account for the

Table 2. Selected Bond Distances (Å) and Angles (deg) for complexes **1** and **2**

	1a (E = S)	**1b** (E = Se)	**2a** (E = S)	**2b** (E = Se)
Co1−E1	2.275(1)	2.3884(9)	2.285(3)	2.3988(6)
Co1−E2	2.261(1)	2.379(1)	2.285(3)	2.4033(6)
E1−Si1	2.114(2)	2.258(2)	2.121(5)	2.258(1)
E2−Si2	2.112(2)	2.251(2)	2.108(5)	2.262(1)
Co1−N1	2.112(4)	2.113(5)	2.075(9)	2.063(3)
Co1−N2	2.122(4)	2.112(5)	2.057(10)	2.057(3)
N2−Co1−N1	86.65(16)	86.8(2)	103.7(2)	99.86(12)
N2−Co1−E1	112.56(11)	108.44(13)	106.9(3)	110.91(9)
N1−Co1−E1	108.44(11)	112.98(13)	102.9(3)	102.83(9)
N2−Co1−E2	104.22(10)	114.39(13)	103.3(3)	104.73(9)
N1−Co1−E2	114.17(11)	104.38(13)	108.1(3)	108.60(9)
E1−Co1−E2	124.31(5)	123.69(4)	129.48(7)	126.75(2)
Si1−E1−Co1	104.65(6)	102.54(5)	105.88(16)	106.17(3)
Si2−E2−Co1	108.51(7)	105.56(5)	107.60(17)	101.30(3)

(14) Komuro, T.; Kawaguchi, H.; Tatsumi, K. *Inorg. Chem.* **2002**, *41*, 5083–5090.
(15) Corwin, D. T.; Gruff, E. S.; Koch, S. A. *J. Chem. Soc., Chem. Commun.* **1987**, *13*, 966–967.
(16) Sobota, P.; Utko, J.; Szafert, S.; Janas, Z.; Glowiak, T. *J. Chem. Soc. Dalton. Trans.* **1996**, *16*, 3469–3473.

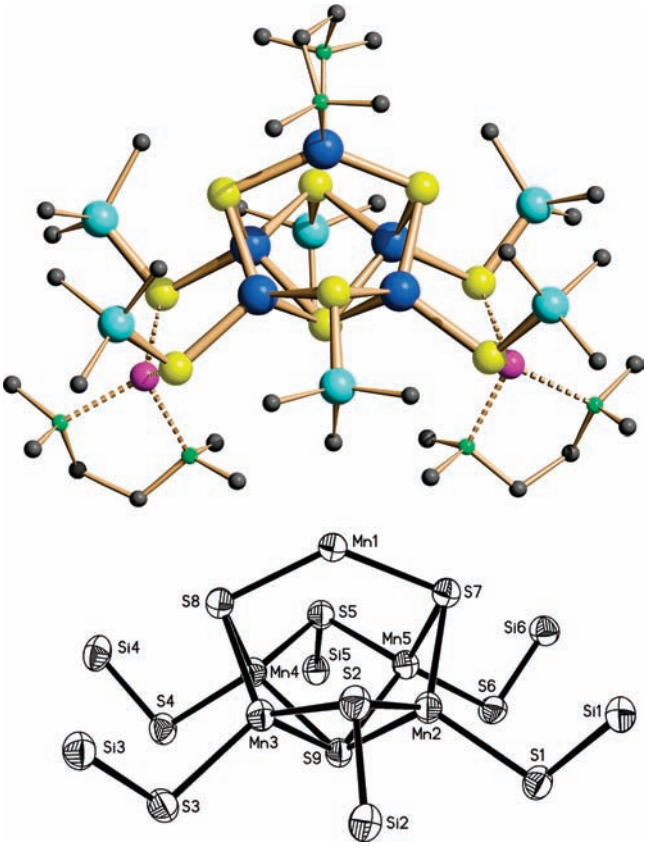

Figure 3. Molecular structure of $[Li(tmeda)]_2[(tmeda)Mn_5(\mu\text{-}SSiMe_3)_2(SSiMe_3)_4(\mu_4\text{-}S)(\mu_3\text{-}S)_2]$ (**3a**; top, hydrogen atoms omitted). Mn, blue; S, yellow; Si, aqua; Li, violet; N, green; C, gray. Bottom: Mn_5S_9 framework in **3a** with the numbering system used (thermal ellipsoids drawn at 40%).

preferred formation of the polynuclear species under these reaction conditions.

$$5MnCl_2 + 9Li[ESiMe_3] + 7.5tmeda \rightarrow [Li(tmeda)]_2[(tmeda)Mn_5(ESiMe_3)_6(E)_3] + 7LiCl + 3ClSiMe_3 + 4.5tmeda\ (E = S, \mathbf{3a}; E = Se, \mathbf{3b}) \quad (1)$$

A summary of the crystal data is listed in Table 1 for **3a** and **3b**. The cluster **3a** crystallizes in the monoclinic space group $P2_1/c$, whereas **3b** crystallizes in the space group $C2/c$, a 2-fold rotation axis along the Mn1−Se5 vector relating the two halves of the molecule. Clusters **3a** and **3b** are structurally similar and are illustrated in Figures 3 and 4, respectively. The structural features common to both complexes include the presence of six trimethylsilylchalcogenolate ligands as well as three bridging chalcogenides. The defined M_5E_3 core, with five manganeses linked via the bridging chalcogenide ligands, is unprecedented in Mn−chalcogenide cluster chemistry. The chalcogenide ligands exhibit both μ_3 and μ_4 bridging modes, and there are two symmetrical bridging μ_2 and four terminal $-ESiMe_3$ ligands. The presence of two tmeda ligated Li ions together with the magnetic susceptibility measurements (*vide infra*) suggest five Mn(II) centers with an overall charge on the cluster of −2. The five Mn(II)'s define a square pyramid and feature a common distorted tetrahedral ME_4 geometry around each metal center; the

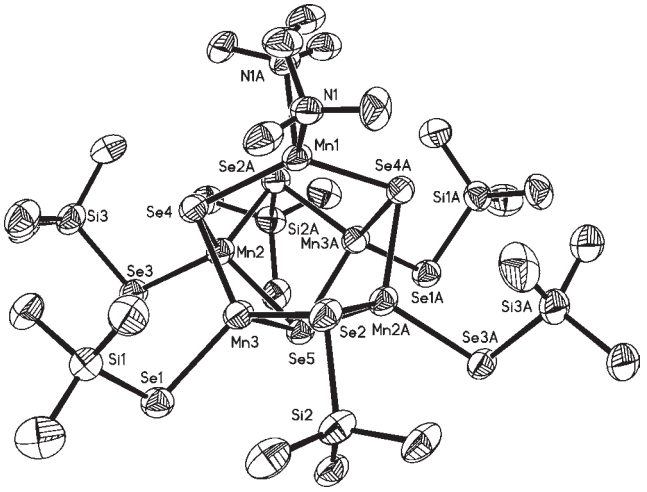

Figure 4. Mn_5Se_9 framework in the molecular structure of $[(tmeda)Mn_5(\mu\text{-}SeSiMe_3)_2(SeSiMe_3)_4(\mu_4\text{-}Se)(\mu_3\text{-}Se)_2]^{2-}$ (**3b**) with the numbering system used (thermal ellipsoids drawn at 40%).

angles about the manganese centers deviate significantly from 109.5°, ranging from 99.80(4) to 132.33(5), as summarized in Table 3. The average Mn−sulfide (2.440(4) Å) and Mn−thiolate (2.440(4) Å) bond lengths are, expectedly, shorter than the average Mn−selenide (2.566(3) Å) and Mn−selenolate (2.559(2) Å) bonding interactions (Table 3). The μ_2-$SSiMe_3$ and μ_2-$SeSiMe_3$ bond lengths are similar to those observed in the adamantoid complexes $[Mn_4(SPr^i)_6)Cl_4]^{2-}$ and $[Mn_4(SePr^i)_6)Br_4]^{2-}$.[17] In **3**, the two Li ions are sequestered, each bonded with one tmeda ligand and further bonded to available lone pairs from two $-ESiMe_3$ ligands (Figure 3). The Mn···Mn distances of adjacent metal centers in **3a** range from 2.960(2) to 3.079(2) Å, whereas they are slightly expanded in the heavier congener **3b** (3.062(3) to 3.151(3) Å). That both **3a** and **3b** contain six trimethylsilylchalcogenolate ($-ESiMe_3$) groups suggests the potential to utilize these complexes as precursors for the synthesis of ternary clusters.[2,4,9]

With the addition of four equivalents of $Li[SSiMe_3]$, there was no evidence for the formation of the pentanuclear complex **3a**, and the mononuclear complex $[Li(tmeda)]_2[Mn(SSiMe_3)_4]$ (**4**) was formed in good yield as the sole product isolated. Single crystal X-ray diffraction confirmed the monomeric nature of the complex, which is illustrated in Figure 5.

$$MnCl_2 + 4Li[SSiMe_3] + 2.5tmeda \rightarrow [Li(tmeda)]_2[Mn(SSiMe_3)_4]4 + 2LiCl + 0.5tmeda \quad (2)$$

The tetrathiolate **4** crystallizes in the tetragonal space group $P4(1)$ (Table 1). Distorted tetrahedral geometry is again observed where the angles about Mn1 range from 95.46(4) to 117.13(5) (Table 4). The magnitude of this asymmetric arrangement around Mn is more pronounced than that observed in $[Et_4N]_2[Mn(S\text{-}2\text{-}Ph{-}C_6H_4)_4]$.[18] The smallest angles (S1−Mn1−S2 and S3−Mn1−S4, 98.12(4)

(17) Stephan, H. O.; Henkel, G. *Polyhedron* **1996**, *15*, 501–511.
(18) Silver, A.; Koch, S. A.; Millar, M. *Inorg. Chim. Acta* **1993**, *205*, 9–14.

Table 3. Selected Bond Distances (Å) and Angles (deg) for Complexes **3a** and **3b**

3a				**3b**	
Mn1−S7	2.3628(12)	S8−Mn3−S2	113.66(4)	Mn1−Se4A	2.4919(7)
Mn1−S8	2.3677(12)	S3−Mn3−S2	114.48(5)	Mn2−Se2A	2.5854(11)
Mn2−S7	2.4066(12)	S8−Mn3−S9	100.60(4)	Se1−Mn3	2.5291(11)
Mn2−S1	2.4227(12)	S3−Mn3−S9	111.02(4)	Se2−Mn3	2.5798(10)
Mn2−S2	2.4686(12)	S2−Mn3−S9	101.05(4)	Se2−Mn2A	2.5854(11)
Mn2−S9	2.5010(12)	S4−Mn4−S(8)	111.77(4)	Se3−Mn2	2.5431(10)
Mn3−S8	2.4178(12)	S4−Mn4−S5	115.84(5)	Se4−Mn1	2.4919(7)
Mn3−S3	2.4163(13)	S8−Mn4−S5	113.72(4)	Se4−Mn3	2.5245(10)
Mn3−S2	2.4729(12)	S4−Mn4−S9	111.96(4)	Se4−Mn2	2.5287(11)
Mn3−S9	2.5057(12)	S8−Mn4−S9	100.85(4)	Mn3−Se5	2.6140(10)
Mn4−S4	2.4079(12)	S5−Mn4−S9	101.13(4)	Mn3A−Se5	2.6140(10)
Mn4−S8	2.4120(12)	S6−Mn5−S7	112.01(5)	Mn2A-Se5	2.6311(9)
Mn4−S5	2.4557(13)	S6−Mn5−S5	116.30(5)	Mn2−Se5	2.6311(9)
Mn4−S9	2.5027(12)	S7−Mn5−S5	113.38(4)	Se4A−Mn1−Se4	132.33(5)
Mn5−S6	2.4154(12)	S6−Mn5−S9	112.73(4)	Se4−Mn2−Se3	111.81(4)
Mn5−S7	2.4137(12)	S7−Mn5−S9	99.80(4)	Se4−Mn2−Se2A	112.00(4)
Mn5−S5	2.4621(13)	S5−Mn5−S9	100.84(4)	Se3−Mn2−Se2A	114.14(4)
Mn5−S9	2.5067(12)			Se4−Mn2−Se5	102.19(3)
S7−Mn1−S8	131.69(4)			Se3−Mn2−Se5	112.85(4)
S7−Mn2−S1	113.50(4)			Se2A−Mn2−Se5	102.90(3)
S7−Mn2−S2	112.67(4)			Se4−Mn3−Se1	113.98(4)
S1−Mn2−S2	114.94(4)			Se4−Mn3−Se2	111.94(4)
S7−Mn2−S9	100.16(4)			Se1−Mn3−Se2	114.16(4)
S1−Mn2−S9	112.62(4)			Se4−Mn3−Se5	102.78(3)
S2−Mn2−S9	101.30(4)			Se1−Mn3−Se5	109.21(4)
S8−Mn3−S3	114.21(4)			Se2−Mn3−Se5	103.53(3)

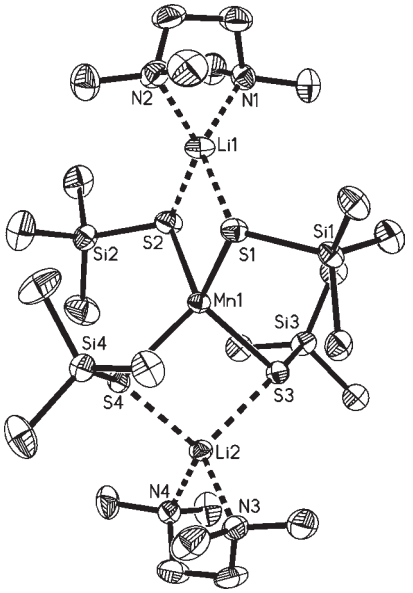

Figure 5. Molecular structure of $[Li(tmeda)]_2[Mn(SSiMe_3)_4]$ (**4**). Thermal ellipsoids are drawn at 40% probability, and H atoms are omitted for clarity.

and 95.46(4)°, respectively) arise from the interaction of the two Li ions to two sulfur sites each. The average Mn−S bond distance (2.441(3) Å) in **4** is comparable to that observed in $[Mn(S\text{-}2\text{-}Ph{-}C_6H_4)_4]^{2-}$ (2.430(3) Å).[18]

Similar reaction conditions used for the preparation of **4** using four equivalents of the selenium reagent Li[$SeSiMe_3$] did not lead to the isolation of a related tetraselenolate complex. The addition of $MnCl_2$(tmeda) to four equivalents of Li[$SeSiMe_3$] resulted in an immediate darkening of the reaction solutions from which orange-red $[Li(tmeda)]_4[Mn_4(SeSiMe_3)_4(\mu_3\text{-}Se)_4]$ (**5**) and dark-red $[Li(tmeda)]_4[Mn(Se_4)_3]$ (**6**) were isolated as single crystals. A summary of the crystal data for complexes **5** and **6** is listed in Table 1.

Table 4. Selected Bond Distances (Å) and Angles (deg) for **4**

Mn1−S1	2.4519(12)	S3−Mn1−S1	117.13(5)
Mn1−S2	2.4468(13)	S4−Mn1−S1	116.11(5)
Mn1−S3	2.4313(14)	S4−Mn1−S2	114.56(5)
Mn1−S4	2.4342(14)	S3−Mn1−S2	116.78(5)
S−Si(avg)	2.106(4)	S3−Mn1−S4	95.46(4)
Li−N (avg)	2.098(18)	S1−Mn1−S2	98.12(4)
Li1−S1	2.462(8)	S1−Li1−S2	93.8(2)
Li1−S2	2.468(8)	N1−Li1−N2	86.9(3)
Li2−S3	2.447(7)	S3−Li2−S4	98.5(2)
Li2−S4	2.439(7)	N3−Li2−N4	87.7(3)

Compound **5** crystallizes in the tricinic space group $P\bar{1}$. The structure of **5** (Figure 6) comprises a tetranuclear cubane $[Mn_4(\mu_3\text{-}Se)_4]$ core, with four Mn and four selenido ligands occupying alternate vertices of the cube. A distorted tetrahedral coordination geometry about the metals is completed with four $-SeSiMe_3$ ligands. This cubane structural motif is common to metal−chalcogenide (O/S/Se/Te) M_4 clusters and has been well investigated due in part to its structural relevance in biological systems.[19] Documented tetranuclear selenido clusters with a cubane-type M_4Se_4 core include those containing the metals Rh, Ir, Co, Fe, and Ru.[2b,20] A manganese(II) cubane cluster with μ_3-oxo ligands has also been prepared,[21] and related telluride−chalcogenolato complexes $[Mn_4Te_4(EPr\textit{i})_4]^{4-}$ (E = S, Se, Te)[22] have been

(19) (a) Krebs, B.; Henkel, G. *Angew. Chem., Int. Ed. Engl.* **1991**, *30*, 769–788. (b) Henkel, G.; Krebs, B. *Chem. Rev.* **2004**, *104*, 801–824.

(20) (a) Seino, H.; Mizobe, Y.; Hidai, M. *Organometallics* **2000**, *19*, 3631–3639. (b) Seino, H.; Mizobe, Y.; Hidai, M. *New J. Chem.* **2000**, *24*, 907–911. (c) Christou, G.; Ridge, B.; Rydon, H. N. *J. Chem. Soc., Dalton Trans.* **1978**, 1423–1425. (d) Kern, A.; Nather, C.; Studt, F.; Tuczek, F. *Inorg. Chem.* **2004**, *43*, 5003–5010.

(21) (a) Shiga, T.; Oshio, H. *Sci. Tech. Adv. Mater.* **2005**, *5*, 565–570. (b) Stoumpos, C. C; Gass, I.; Milios, C. J.; Kefallaniti, E.; Raptopoulou, C. P.; Terzis, A.; Lalioti, N.; Brechin, E. K.; Perlepes, S. P *Inorg. Chem. Commun.* **2008**, *11*, 196–202.

(22) (a) Stephan, H. O.; Henkel, G. *Angew. Chem., Int. Ed. Engl.* **1994**, *33*, 2322–2324. (b) Stephan, H. O.; Chen, C.; Griesar, K.; Haase, W.; Henkel, G. *J. Chem Soc., Chem.Commun.* **1993**, *10*, 886–888.

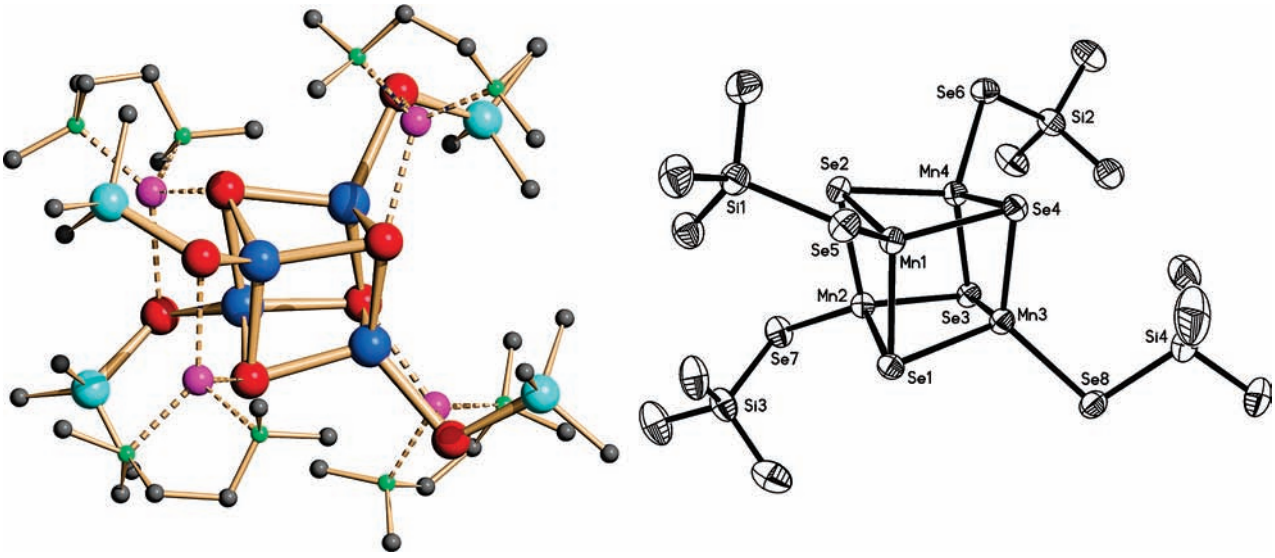

Figure 6. Molecular structure of $[Li(tmeda)]_4[Mn_4(SeSiMe_3)_4(\mu_3\text{-}Se)_4]$ (**5**; left, hydrogen atoms omitted). Mn, blue; Se, red; Si, aqua; Li, violet; N, green; C, gray. (Right) The Mn_4Se_8 framework in **5** with numbering used (thermal ellipsoids drawn at 40%).

reported by Henkel and co-workers. To our knowledge, this is the first example of a structurally characterized tetranuclear manganese selenium cluster displaying this structural motif. The Mn_4Se_4 core in **5** is distorted from an ideal cubic geometry as indicated by the variation of Mn−Se bond distances (Table 5) and the endohedral angles of the Mn_4Se_4 core. Although there are numerous reports on the incorporation of Mn(II) centers into mixed metal MnM_3E_4 (M = transition metal) clusters, the polynuclear complex **5** represents the first example of a homometallic Mn_4Se_4 complex with a cubane core. The selenide ligands in **5** each symmetrically bridge three Mn(II) sites with the tetrahedral coordination geometry about the metals completed with the $-SeSiMe_3$ (Table 5). The Mn···Mn distances in **5** (3.087(1) to 3.180(1) Å) are contracted compared to those in the telluride/tellorolate complex $[Mn_4Te_4(EPr^i)_4]^{4-}$ (3.214(4) to 3.358(4) Å).[22] In contrast to this cubane framework, the polynuclear manganese selenides recently reported by Eichhöfer display adamantane-based structures.[23] In **5**, four TMEDA ligated Li^+'s serve as the counterions present in the crystal for the $[Mn_4(SeSiMe_3)_4(\mu_3\text{-}Se)_4]^{4-}$ frame. These Li ions each also form two additional contacts with the Se centers of the trimethylsilylselenolate ligands. The resultant formulation of the cluster with four Mn(II)'s is consistent with the magnetic measurements (*vide infra*). There is no clear relationship between the structural features of the metal−chalcogen core in **5** and that of the pentamanganese complex **3b**.

In addition to the isolation of $[Li(tmeda)]_4[Mn_4(SeSiMe_3)_4(\mu_3\text{-}Se)_4]$ (**5**), small amounts of dark red crystals were also present from these reactions. A single crystal X-ray analysis indicated the formation of the tris(tetraselenide complex) $[Li(tmeda)]_4[Mn(Se_4)_3]$ (**6**). Compound **6** crystallizes in the monoclinic space group $P2(1)/n$. The structure of **6** (Figure 7) consists of a Mn(II) center chelated by three tetraselenide ligands, $(Se_4)^{2-}$ with a distorted octahedral geometry around the central metal.

Table 5. Bond Distances (Å) and Angles (deg) for **5**

Mn(1)−Se(2)	2.5387(10)	Mn(2)−Mn(4)	3.0874(12)
Mn(1)−Se(5)	2.5447(9)	Mn(2)−Mn(3)	3.2171(12)
Mn(1)−Se(4)	2.5716(10)	Mn(3)−Se(4)	2.5326(10)
Mn(1)−Se(1)	2.5944(10)	Mn(3)−Se(8)	2.5424(10)
Mn(1)−Mn(3)	3.1192(11)	Mn(3)−Se(1)	2.5758(10)
Mn(1)−Mn(2)	3.1488(12)	Mn(3)−Se(3)	2.6280(10)
Mn(1)−Mn(4)	3.1801(11)	Mn(3)−Mn(4)	3.1165(12)
Mn(2)−Se(7)	2.5464(11)	Mn(4)−Se(3)	2.5169(9)
Mn(2)−Se(1)	2.5495(10)	Mn(4)−Se(6)	2.5270(10)
Mn(2)−Se(3)	2.5738(10)	Mn(4)−Se(2)	2.5559(10)
Mn(2)−Se(2)	2.5956(10)	Mn(4)−Se(4)	2.6112(10)
Se2−Mn1−Se5	122.75(4)	Se4−Mn3−Se8	122.71(4)
Se2−Mn1−Se4	101.59(3)	Se4−Mn3−Se1	104.90(3)
Se5−Mn1−Se4	115.99(4)	Se8−Mn3−Se1	114.71(4)
Se2−Mn1−Se1	103.20(3)	Se4−Mn3−Se3	103.47(3)
Se5−Mn1−Se1	107.82(3)	Se8−Mn3−Se3	108.72(3)
Se4−Mn1−Se1	103.26(3)	Se1−Mn3−Se3	99.33(3)
Se7−Mn2−Se1	126.33(4)	Se3−Mn4−Se6	125.22(4)
Se7−Mn2−Se3	114.22(4)	Se3−Mn4−Se2	106.04(3)
Se1−Mn2−Se3	101.48(3)	Se6−Mn4−Se2	109.59(4)
Se7−Mn2−Se2	106.09(4)	Se3−Mn4−Se4	104.39(3)
Se1−Mn2−Se2	102.87(3)	Se6−Mn4−Se4	108.64(4)
Se3−Mn2−Se2	103.24(3)	Se2−Mn4−Se4	100.05(3)

The Mn−Se bond lengths vary from 2.647(2) to 2.798(1), each pair of Mn−Se lengths associated with a Se_4 ring displaying one shorter (2.647(2)−2.700(2) Å) and one longer (2.767(2)−2.798(2) Å) bond (Table 6). These bond lengths are themselves longer than those reported in the tetrahedral bis(tetraselenide) manganese complex $[Mn(Se_4)_2]^{2-}$ (2.537(5)−2.553(5) Å).[24] $[Pt(Se_4)_3]^{2-}$,[25] $[Ir(Se_4)_3]^{3-}$,[26] and $[Sn(Se_4)_3]^{2-}$ [24,27] represent other examples of structurally characterized octahedral selenometalates containing three tetraselenide ligands. The origin for the reproducible formation of **6** in the reaction is unclear but requires partial

(23) Eichhöfer, A.; Wood, P. T.; Viswanath, R. N.; Mole, R. A. *Chem. Commun.* **2008**, *13*, 1596–1598.

(24) Huang, S. P.; Dhingra, S.; Kanatzidis, M. G. *Polyhedron* **1990**, *9*, 1389–1395.

(25) (a) Ansari, M. A.; Ibers, J. A. *Inorg. Chem.* **1989**, *28*, 4068–4069. (b) McConnachie, J. M.; Ansari, M. A.; Ibers, J. A. *Inorg. Chem.* **1993**, *32*, 3250–3255.

(26) (a) Albrecht-Schmitt, T. E.; Cody, J. A.; Hupp, J. T.; Ibers, J. A. *Inorg. Chem.* **1995**, *34*, 5101–5102. (b) Albrecht-Schmitt, T. E.; Ibers, J. A. *Inorg. Chem.* **1996**, *35*, 7273–7278.

(27) Banda, R. M. H.; Cusick, J.; Scudder, M. L.; Craig, D. C.; Dance, I. G. *Polyhedron* **1989**, *8*, 1999–2001.

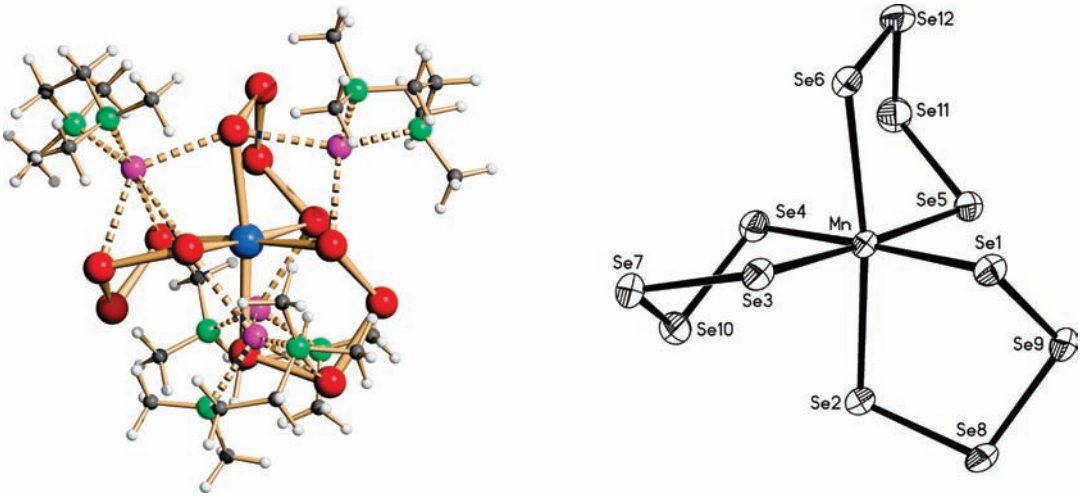

Figure 7. Structure of $[Li(tmeda)]_4[Mn(Se_4)_3]$ (**6**; left). Mn, blue; Se, red; Li, violet; N, green; C, gray; H, white. (Right) The $[Mn(Se_4)_3]^{4-}$ structure in **6** with numbering used (thermal ellipsoids drawn at 40%).

Table 6. Bond Lengths (Å) and Angles (deg) for **6**

Mn−Se1	2.700(2)	Se1−Mn−Se5	89.57(5)
Mn−Se2	2.798(1)	Se2−Mn−Se3	91.70(4)
Mn−Se3	2.767(2)	Se2−Mn−Se4	85.60(5)
Mn−Se4	2.647(2)	Se2−Mn−Se5	94.84(4)
Mn−Se5	2.685(1)	Se4−Mn−Se5	92.35(5))
Mn−Se6	2.782(1)	Se3−Mn−Se4	95.44(5)
Se1−Mn−Se2	93.09(5)	Se3−Mn−Se6	82.14(4)
Se1−Mn−Se3	82.77(5)	Se4−Mn−Se6	90.15(5)
Se1−Mn−Se6	90.94(5)	Se5−Mn−Se6	91.90(4)

oxidation of Se^{2-} species present in the reaction. ^{77}Se NMR spectra of solutions of prepared $Li[SeSiMe_3]$ display only one resonance at −518 ppm, with no evidence for any tetraselenide species being present.[28]

The temperature dependent magnetic susceptibilities of the clusters **3a**, **3b**, and **5** were measured on polycrystalline samples using a SQUID magnetometer. The results for compound **3a** are presented in Figure 8 as plots of χT vs T and M vs H. At room temperature, the χT product for **3a** is 5.69 cm^3 K mol^{-1}, a much lower value than the calculated one (21.875 cm^3 K mol^{-1}) for five spin-only Mn(II) centers ($S = 5/2$, $g = 2$, $C = 4.375$ cm^3 K mol^{-1}). This type of behavior is indicative of very strong overall antiferromagnetic interactions within this square pyramidal Mn_5 core. This is supported by the temperature dependence of the χT product at 1000 Oe, which continuously decreases down to a plateau at 2.36 cm^3 K mol^{-1} at ∼3.5 K until 1.8 K. The observed χT value of 2.36 cm^3 K mol^{-1} is compatible with a total spin ground state between $S = 3/2$ (1.875 cm^3 K mol^{-1}) and 2 (3.0 cm^3 K mol^{-1}). Analyzing the spin topology within the structure, the four Mn(II) ions in the basal square plane are expected to be antiferromagnetically coupled through the chalcogen bridges, and thus the total spin ground state of the compound would be 5/2, contributed by the lone Mn(II) located above the Mn_4 plane. Therefore, the theoretical χT value at 1.8 K should be 4.375 cm^3 K mol^{-1} and the magnitude of the magnetization 5 μ_B, which are values in close agreement with the experimentally observed χT value (2.36 cm^3 K mol^{-1}) at 1.8 K and magnetization (3.1 μ_B) at 7 T and 1.8 K. We attribute the discrepancies to the extreme air sensitivity of the samples, resulting in the slight oxidation of Mn(II) ions. As illustrated in Figure S1 (Supporting Information), the temperature-dependent magnetic susceptibility and the magnetization of the selenium complex **3b** show similar data sets to those of **3a** due to their structural similarities.

At room temperature, the observed χT value for the Mn_4 complex **5** is 4.08 cm^3 K mol^{-1}, much lower in comparison to the calculated one (17.5 cm^3 K mol^{-1}) for four Mn(II) centers (Figure 9, left). Again, the very low room temperature χT product indicates the presence of very strong overall antiferromagnetic interactions within the tetranuclear metallic core. This is confirmed by the temperature dependence of the χT product at 1000 Oe that continuously decreases down to 0.52 cm^3 K mol^{-1} until 1.8 K, compatible with a total spin ground state of $S = 1/2$ (0.375 cm^3 K mol^{-1}). However, the field dependence of the magnetization at low temperatures as shown in Figure 9 (right) indicates that the magnetization is only slightly populated with an increase of the applied DC field, suggesting that the total spin ground state of this compound is zero. This discrepancy in the results can again be attributed to the extreme air sensitivity of the sample, leading to partial oxidation during sample transfer. Taking into consideration the structure, antiferromagnetic couplings between the four Mn(II) centers would lead to a total spin ground state of zero. The overall magnetic behavior indicates the presence of dominant antiferromagnetic interactions within this tetranuclear Mn(II) compound, as reported for $[Mn_4Te_4(TePr^i)_4]^{4-}$ and related manganese−chalcogen polynuclear complexes.[22b,23,29]

Conclusion

We have been able to synthesize and characterize Mn(II) and Co(II) complexes with trimethylsilylchalcogenolate ligands. The X-ray crystallographic analysis of these complexes shows the presence of potentially reactive $-ESiMe_3$

(28) Cusick, J.; Dance, I. *Polyhedron* **1991**, *10*, 2629–2640.

(29) (a) Stephan, H. O.; Kanatzidis, M. G; Henkel, G. *Angew. Chem., Int. Ed. Engl.* **1996**, *35*, 2135–2137. (b) Eichhöfer, A.; Wood, P. T.; Viswanath, R. N.; Mole, R. A. *Eur. J. Inorg. Chem.* **2007**, *30*, 4794–4799. (c) Mellullis, M.; Clerac, R; Dehnen, S. *Chem. Commun.* **2005**, *48*, 6008–6010.

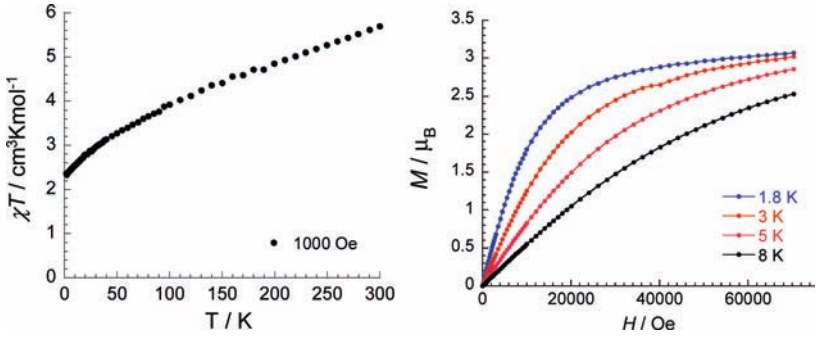

Figure 8. Plots of χT vs T (left) and M vs H (right) for complex **3a**.

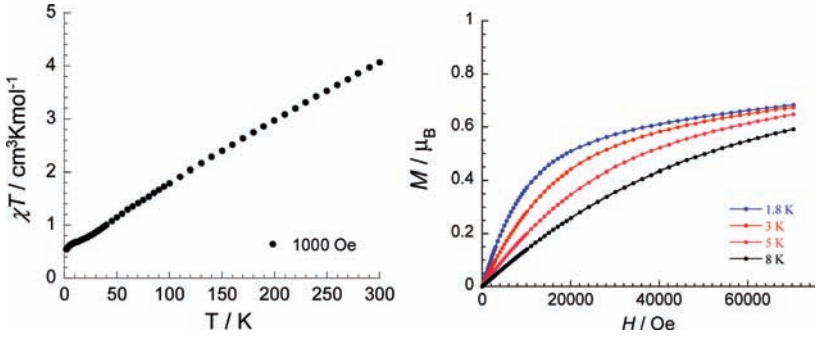

Figure 9. Plots of χT vs T (left) and M vs H (right) for complex **5**.

moieties and suggests that these compounds could potentially be utilized as precursors to the ternary nanocluster synthesis. These compounds should be a convenient source of paramagnetic ions into a semiconductor matrix for the synthesis of ternary clusters that could potentially manifest magnetic as well as semiconducting properties. The reactions to test the utility of these precursors for nanocluster preparation are underway.

Acknowledgment. We gratefully acknowledge the Natural Sciences and Engineering Research Council of Canada (N.S.E.R.C.) for financial support of this research and equipment funding. The Government of Ontario, The University of Western Ontario (U. W. O.), and the Canada Foundation for Innovation are thanked for equipment funding. J.F.C. thanks the Center for Functional Nanostructures (Universität Karlsruhe) for support via a visiting professorship. C.B.K. gratefully acknowledges the ASPIRE program at U. W. O. for travel support.

Supporting Information Available: Crystallographic information files (CIF) for complexes **1**−**6** and plots of χT vs T and M vs H for complex **3b.** This material is available free of charge via the Internet at http://pubs.acs.org.